Journal of Nuclear Science and Technology

ISSN: 0022-3131 (Print) 1881-1248 (Online) Journal homepage: https://www.tandfonline.com/loi/tnst20

Simple Electrolyzer Model Development for High-Temperature Electrolysis System Analysis Using Solid Oxide Electrolysis Cell

JaeHwa KOH , DuckJoo YOON & Chang H. OH

To cite this article: JaeHwa KOH , DuckJoo YOON & Chang H. OH (2010) Simple Electrolyzer Model Development for High-Temperature Electrolysis System Analysis Using Solid Oxide Electrolysis Cell, Journal of Nuclear Science and Technology, 47:7, 599-607

To link to this article: https://doi.org/10.1080/18811248.2010.9720957

Published online: 05 Jan 2012.

Journal of NUCLEAR SCIENCE and TECHNOLOGY, Vol. 47, No. 7, p. 599–607 (2010)

ARTICLE

Simple Electrolyzer Model Development for High-Temperature Electrolysis System Analysis Using Solid Oxide Electrolysis Cell

JaeHwa KOH[1,*], DuckJoo YOON[1] and Chang H. OH[2]

[1]*KEPCO Research Institute, 65, Munji-Ro, Yuseong-Gu, Daejeon 305-760, Korea*
[2]*Idaho National Laboratory, 2525 N. Fremont Ave., Idaho Falls, ID 83415, USA*

(Received September 14, 2009 and accepted in revised form February 23, 2010)

An electrolyzer model for the analysis of a hydrogen production system using a solid oxide electrolysis cell has been developed, and the effects of principal parameters have been estimated via sensitivity studies based on the developed model. The main parameters considered were current density, area-specific resistance, temperature, pressure, molar fraction, and flow rates in the inlet and outlet. A simple model is also estimated for a high-temperature hydrogen production system that integrates the solid oxide electrolysis cell with a very high temperature reactor.

KEYWORDS: high-temperature electrolysis system (HTES), solid oxide electrolysis cell (SOEC), hydrogen production, nuclear hydrogen, electrolyzer, very high temperature reactor (VHTR)

I. Introduction

Due to uncertainties in the future of fossil energy supplies, including coal and natural gas, interest in renewable energy is gradually increasing worldwide. Hydrogen energy is an emerging source that provides future energy. Various methods are currently used to produce hydrogen, but high-temperature electrolysis (HTE), sulfur iodine (SI), and hybrid sulfur[1,2] processes are considered the most promising candidates for producing large quantities. Especially noteworthy, high-temperature electrolysis, which operates at over 800°C, can produce hydrogen efficiently and effectively, providing synergistic effects with current solid oxide fuel cell (SOFC) technology.[3]

The KEPCO Research Institute (KEPRI) began implementing a nuclear hydrogen project using HTE in 2008, and constructed a small lab-scale high-temperature electrolysis system (HTES) in the end of 2009. Before the system was completed, we needed information on cell behavior during the electrolysis reaction with various considerations and preliminary analysis for high-temperature electrolysis system configuration. Firstly, in the course of this study, we implemented an electrolyzer model development and parametric study using the HYSYS process analysis code, which is maintained by Aspen Technology[4] and generally used for process simulation of chemical plants and oil refineries. Previous researchers have tried to develop an HTE model using process analysis codes.[5–9] McKeller *et al.* (2007) developed an electrolyzer model with the UniSim process analysis code, a variation of the HYSYS code.[6] Oh *et al.* (2007) estimated a very high temperature gas-cooled reactor coupled with the high-temperature electrolysis process by using the HYSYS code.[5] When Oh *et al.* (2007) developed the electrolyzer model, he used a triple integral method to calculate the average V_{nernst}, but for the electrolyzer model introduced in this paper, the trapezoidal rule method was applied to calculate the average V_{nernst}.

II. An Electrolyzer Model for High-Temperature Electrolysis System

1. Thermodynamics

The HTES is based on the solid oxide electrolysis cell (SOEC), a reversible reaction involving a solid oxide fuel cell (SOFC). The reactions in the SOEC can be written as follows:

$$\text{Cathode:} \quad H_2O(g) + 2e^- \rightarrow H_2(g) + O^{2-}, \tag{1}$$

$$\text{Anode:} \quad O^{2-} \rightarrow 1/2O_2(g) + 2e^-, \tag{2}$$

$$\text{Total:} \quad H_2O(g) \rightarrow H_2(g) + 1/2O_2(g). \tag{3}$$

The SOEC is generally operated at high temperatures ranging from 750 to 1000°C. Because of the high temperature, H_2O exists in the system as a gas. The following summarizes the basic thermodynamic equations and models used in the HTE.

Required total energy (ΔH) for high-temperature electrolysis of the steam can be expressed as a function of Gibbs free energy (ΔG) and heat energy ($T\Delta S$) as follows:

$$\Delta H = \Delta G + T\Delta S \tag{4}$$

$$\text{(Total Energy)} = \text{(Electrical Energy)} + \text{(Heat Energy)}.$$

*Corresponding author, E-mail: euron@kepri.re.kr

Table 1 Thermodynamic data for HTES at 1 atm and 298.15 K

Substance (state)	ΔH° (kJ/mol)	ΔG° (kJ/mol)	S° (kJ/mol·K)	Heat capacity, Cp° (J/mol·K)
H_2 (gas)	0[10,11]	0[10,11]	0.131[10] 0.130[11]	28.84[10] $27.28 + 0.00326T + 5000/T^2$[12] $(29.07 - 0.836) \times 10^{-3}T + 20.1 \times 10^{-7}T^2$[13]
O_2 (gas)	0[10,11]	0[10,11]	0.205[11]	$29.96 + 0.00418T - 167000/T^2$[12] $(25.72 + 12.98) \times 10^{-3}T - 38.6 \times 10^{-7}T^2$[13]
H_2O (liquid)	237.2[10]	285.8[10]	0.0699[11]	75.35[10] 75.44[12] 75.30[13]
H_2O (gas)	228.6[10]	241.8[10]	0.1888[11]	33.60[10] $30.00 + 0.01071T + 33000/T^2$[6] $(30.36 + 9.61) \times 10^{-3}T + 11.8 \times 10^{-7}T^2$[7]

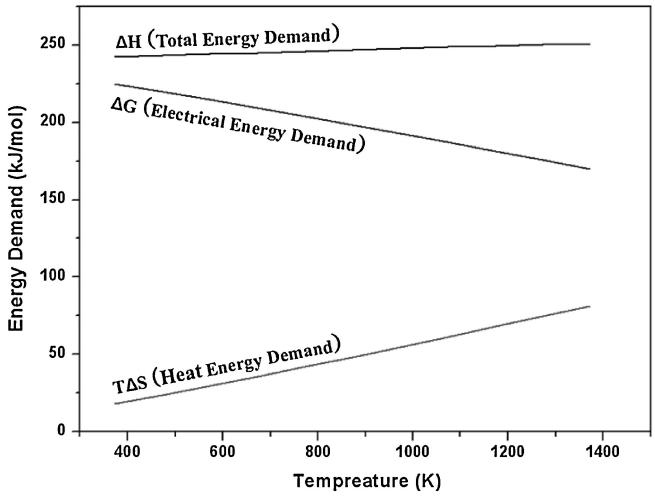

Fig. 1 Total energy demand for hydrogen production

Table 1 shows the standard thermodynamic parameters for HTES at 1 atm and 298.15 K.[10–13] Shin *et al.*[12] and Mingyi *et al.*[13] showed other equations of heat capacity varying as a function of temperature.

Energy demand for HTES is shown in **Fig. 1**. ΔH represents total energy demand, ΔG stands for electrical energy demand, and $T\Delta S$ symbolizes heat energy demand. The minimum electrical energy for electrolysis at 850°C is about 25% less than for electrolysis at room temperature.[14] Also, if the $T\Delta S$ could be provided from thermal energy such as a nuclear heat source, high-temperature electrolysis would theoretically be more efficient.[14] With increasing temperature, the required electrical energy is reduced because of the increase in heat energy (Fig. 1). Heat energy sources for massive hydrogen production can be found in geothermal energy, industrial waste heat energy, and nuclear energy.

2. Electrolyzer Model

This section describes the electrolyzer model developed in this study using the HYSYS process analysis code. Since the HYSYS code does not include the electrolyzer model, an electrolyzer model for HTES analysis was newly developed using other basic system components. **Figure 2** shows the process flow diagram of the electrolyzer model. The electrolyzer model includes one conversion reactor for electrolysis reaction, one component splitter for the separation of H_2 (cathode electrode) and O_2 (anode electrode) flows, many material streams for each material flow, two energy streams for electrical and heat energy, and four SET logical operations for matching temperatures or pressures (Fig. 2). The conversion reactor used a stoichiometry equation to illustrate the splitting of water (status of liquid or steam) and the flow amounts of each product after reaction were determined using the conversion percent. The HYSYS program is used to calculate the heat energy for reaction within a conversion reactor (isothermal electrolysis in Fig. 2) and component splitter (electrode separation in Fig. 2). Gibbs free energy, average V_{nernst} potential, V_{cell} (or V_{op}) potential, electrical power energy, and process heat energy are calculated by spreadsheet calculations within the HYSYS program.

Chemical balance of the electrolysis reaction can be written as $H_2O(g) \rightarrow H_2(g) + 1/2O_2(g)$ from Eq. (3). Gibbs free energy in the above reaction is a function of temperature and pressure and can be written as[5]

$$\Delta G(T,P) = \Delta G_f(T,P) + R \cdot T \cdot \ln\left[\left(\frac{f_{H_2} f_{O_2}^{\frac{1}{2}}}{f_{H_2O}}\right)\right], \quad (5)$$

where

f: molar fraction of a species,
R: gas constant (8.314 J/mol·K),
T: temperature (K).

$\Delta G_f(T,P)$ is the Gibbs free energy for the products at temperature and pressure minus that for the reactants; that is,

$$\Delta G_f(T,P) = G_{f\text{-}H_2}(T,P) + 1/2G_{f\text{-}O_2}(T,P) - G_{f\text{-}H_2O}(T,P). \quad (6)$$

$\Delta G_f(T,P)$ is written in terms of $\Delta G_f^\circ(T,P) = G_f(T,P_{\text{STD}})$, where $P_{\text{STD}} = 0.101$ MPa. The change in Gibbs free energy is equal to the electrical voltage potential required for electrolysis, as in

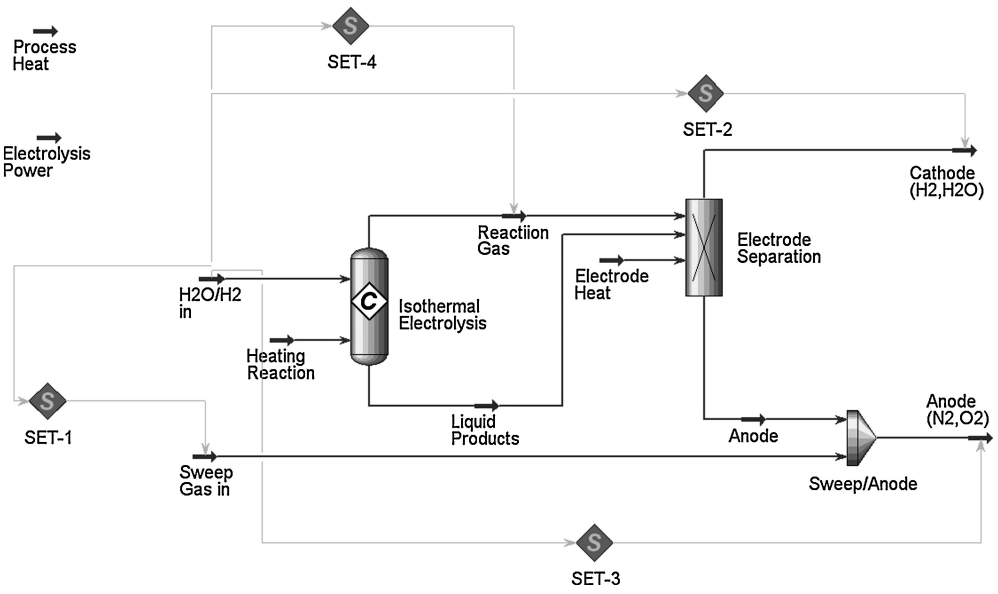

Fig. 2 Process flow diagram of electrolyzer model (HYSYS)

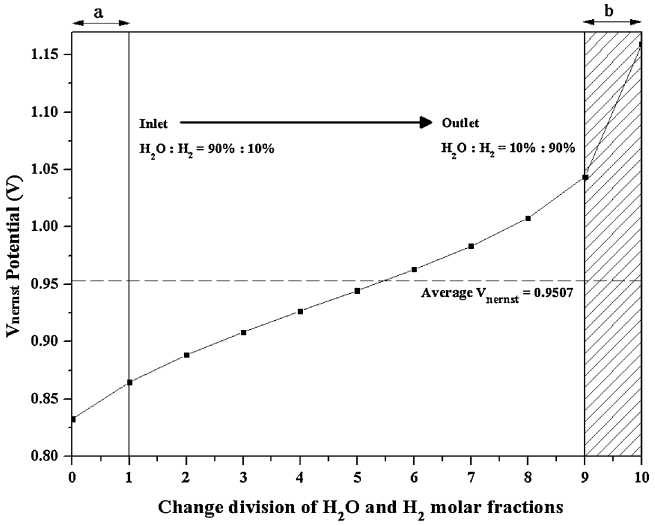

Fig. 3 V_{nernst} potential for H_2O and H_2 molar fractions

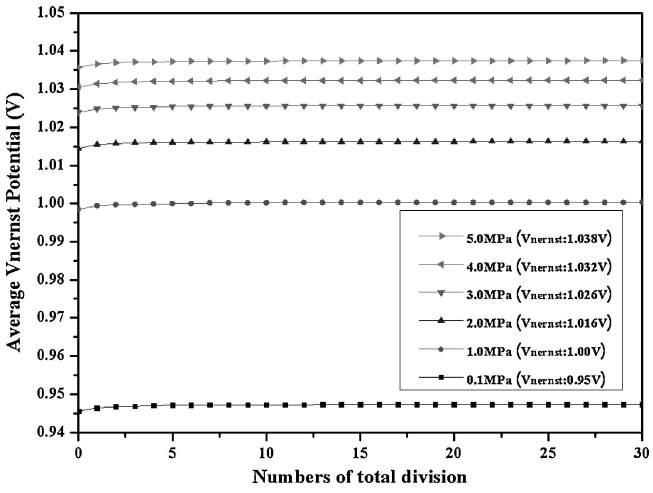

Fig. 4 Convergence of average V_{nernst} potential (MATLAB)

$$V_{\text{nernst}} = \frac{-1}{2\text{F}}\left[\Delta G_{\text{f}}^{\circ}(T,P) - R\cdot T \times \ln\left[\left(\frac{f_{\text{H}_2\text{O}}}{f_{\text{H}_2} f_{\text{O}_2}^{\frac{1}{2}}}\right)\left(\frac{P}{P_{\text{STD}}}\right)^{-\frac{1}{2}}\right]\right] \quad (7)$$

where $P_{\text{STD}} = 0.101\,\text{MPa}$ and P is the cell (or stack) pressure and F is the Faraday constant (96,485 Coulomb/mole). Since the V_{nernst} varies in the electrolyzer depending on the temperature, pressure, and species concentrations, an average V_{nernst} potential has been estimated in the HYSYS spreadsheet. The whole channels were divided into several subregions with the same intervals and numerically averaged.

During the electrolysis reaction, the molar flow and V_{nernst} potential of H_2O (or H_2) was changed in the channel, as shown in **Fig. 3**. When the H_2O molar fraction is lower than 10% (or the H_2 molar fraction is higher than 10%), the slope of V_{nernst} potential rapidly increases (a or b in Fig. 3). Therefore, when the H_2O molar fraction is between 0 and 10%, division into more steps is necessary, and careful calculations of average V_{nernst} potential must be performed.

To reduce more round-off errors for the average V_{nernst} calculation in the electrolyzer model, the trapezoidal rule was finally applied to the V_{nernst} integration as

$$\text{Average } V_{\text{nernst}} = \frac{1}{2n}\left(V_{\text{nernst}_0} + 2\cdot V_{\text{nernst}_1} + 2\cdot V_{\text{nernst}_2} + \cdots + 2\cdot V_{\text{nernst}_{n-1}} + V_{\text{nernst}_n}\right), \quad (8)$$

where

n: number of division steps (in the cell).

If the molar fraction of H_2O or H_2 exists between 10 and 90%, the average V_{nernst} potential can be calculated as the V_{nernst} potential at each divided spot under 20 steps as shown in **Fig. 4**. Therefore, developed electrolyzer models can be used to predict the average V_{nernst} potential between 10 and 90% of the molar fraction.

Table 2 Reference conditions for parametric study

Inlet flow	Sweep gas	Temperature	Pressure	Current density	Area-specific resistance (ASR)
1 gmole/s H_2O: 90% H_2: 10%	0.5 gmole/s N_2: 21% O_2: 79%	1073 K (800°C)	101.325 kPa (1 atm)	0.25 A/cm^2	0.25 Ω·cm^2

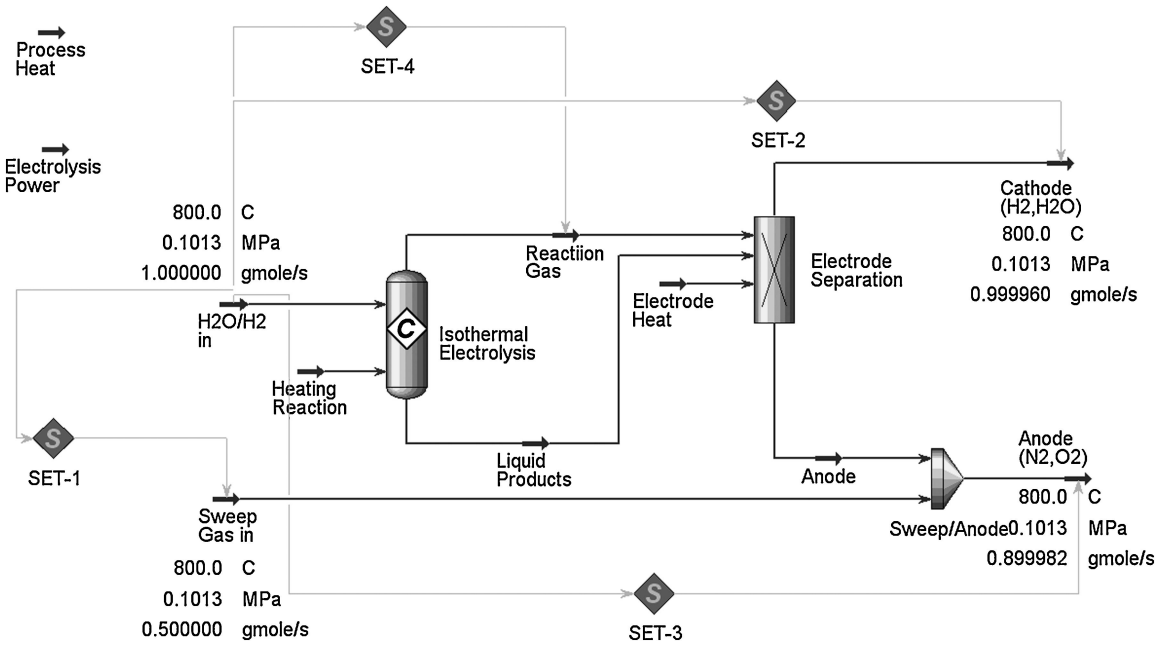

Fig. 5 Process flow diagram for initial condition (HYSYS)

Following calculation of the average V_{nernst} potential, V_{op} or V_{cell} potential, electrical work energy, and process heat energy can be calculated. V_{op} is written as

$$V_{\text{op}} = \text{average } V_{\text{nernst}} + i \cdot ASR, \tag{9}$$

where

i: current density (A/cm^2),
ASR: area-specific resistance (Ω·cm^2).

The electrical work done in the cell is

$$W_{\text{El}} = V_{\text{op}} \cdot I = V_{\text{op}} \cdot i \cdot A, \tag{10}$$

where

I: current (Amperes),
A: area of cell (or stack) (cm^2).

The electrical work is used as the input value of the electrolysis power (within the process flow diagram at the electrolyzer model). An energy balance at the electrolyzer model is written as

$$\sum_i \dot{n}_{\text{P-}i} H_{\text{P-}i}(T_{\text{p}}, P) = \sum_i \dot{n}_{\text{R-}i} H_{\text{R-}i}(T_{\text{R}}, P) + Q_{\text{Heat}} + W_{\text{El}}, \tag{11}$$

where

$\dot{n}$: species molar flow rate (kgmole/s),
H: Enthalpy per mole (kJ/kgmole),
Q_{Heat}: transferred heat energy from outside to the electrolyzer (kW),
W_{El}: transferred electrical energy from outside to the electrolyzer (kW),
T: temperature (°C),
P: pressure (kPa).

The subscript R was used for reactants and P for products. From Eq. (10), we give the required heat energy (Q_{Heat}) in the electrolyzer model as it is calculated using the HYSYS spreadsheet.

$$\begin{aligned} Q_{\text{Heat}} &= [\dot{n}_{\text{H}_2\text{O}} H_{\text{H}_2\text{O}}(T,P) + \dot{n}_{\text{H}_2} H_{\text{H}_2}(T,P) + \dot{n}_{\text{O}_2} H_{\text{O}_2}(T,P)]_{\text{outlet}} \\ &\quad - [\dot{n}_{\text{H}_2\text{O}} H_{\text{H}_2\text{O}}(T,P) + \dot{n}_{\text{H}_2} H_{\text{H}_2}(T,P) + \dot{n}_{\text{O}_2} H_{\text{O}_2}(T,P)]_{\text{inlet}} \\ &\quad - W_{\text{El}} \end{aligned} \tag{12}$$

Both the sum of internal energy and the sum of external energy are the same and balanced by spreadsheet calculation within the HYSYS code automatically.

3. Parametric Study on the Electrolyzer Model

Parametric studies were preformed on the developed electrolyzer model in order to understand its characteristics. **Table 2** summarizes the reference conditions for the based case assumed in this analysis. This condition was applied as

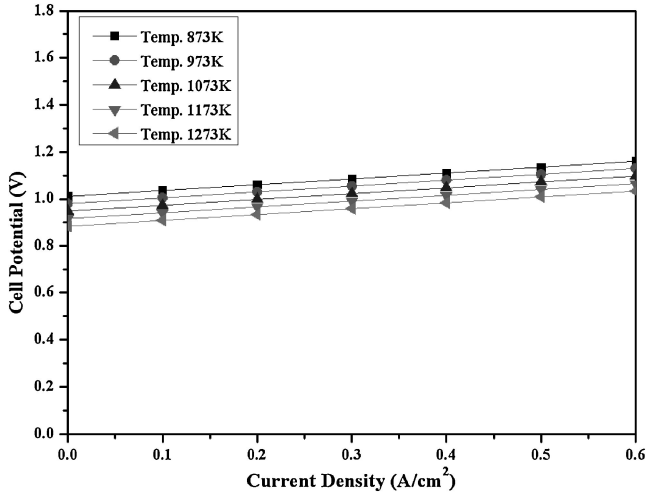

Fig. 6 Cell potential effect for current density and temperature

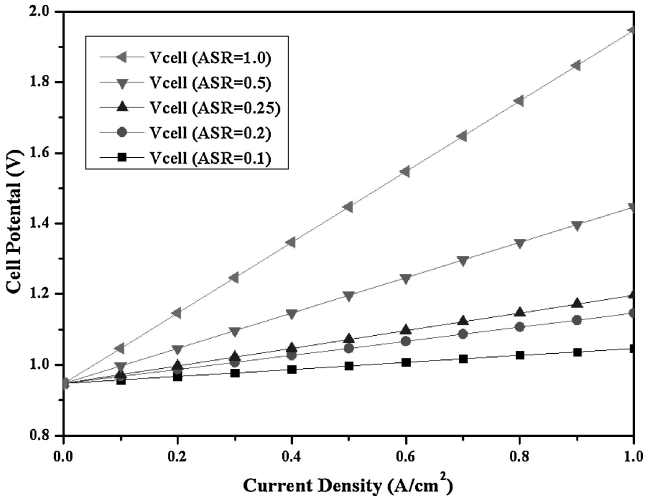

Fig. 8 Cell potential effect for cell density and ASR

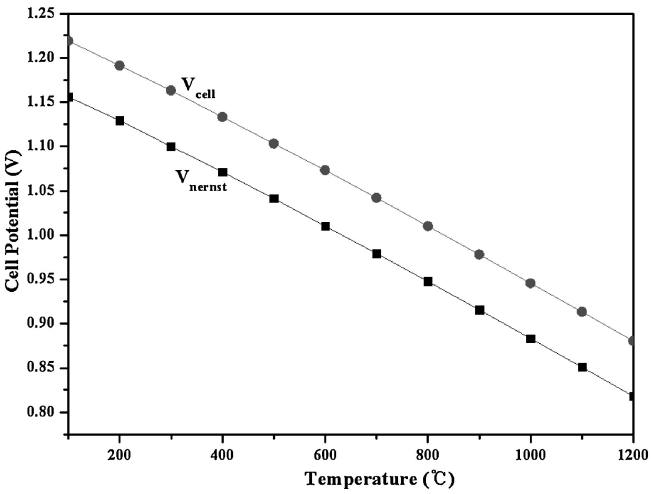

Fig. 7 Cell potential effect for temperature

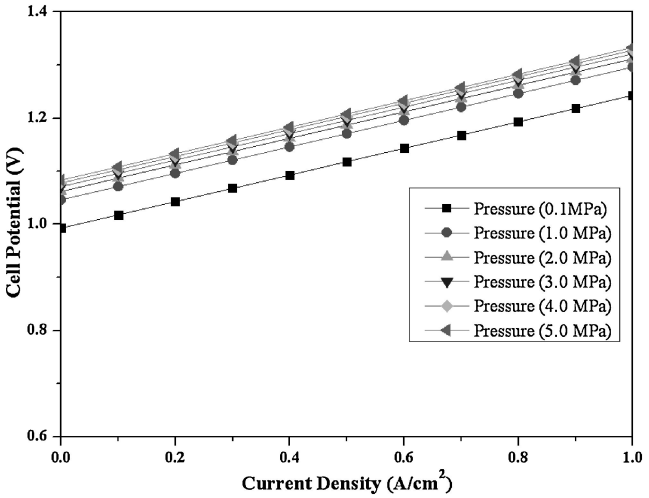

Fig. 9 Cell potential effect for current density and pressure

input to the developed electrolyzer model as shown in **Fig. 5**. The parameters taken into consideration for the parametric studies were (1) temperature, (2) current density, (3) area-specific resistance (ASR), (4) molar or mass flow rate in the inlet side, and (5) molar or mass fraction of each species in the inlet side. These parameters are briefly discussed below.

(1) Effects of Current Density, Temperature and ASR on the Cell Potential

The cell potential increases with the increase in current density, as shown in **Fig. 6**, and decreases as temperature increases, as shown in **Fig. 7**. Cell potential is a function of temperature, current density, and area-specific resistance, as shown in Eq. (8). When the value of current density is 0 (zero), the cell potential is determined using average V_{nernst}.

In the electrochemical reaction, ASR is a function of temperature and varies based on experimental conditions and the material of the cell (or stack). Therefore, if the temperature at the same current density varies, the cell potential is also different. The cell potential rapidly increases with ASR under the same current density conditions, as shown in **Fig. 8**. For a more detailed simulation, ASR should be changed as an estimated value from the HTE experiment. ASR is assumed as constant in this electrolyzer model; *i.e.*, current density (i) and ASR are used as the input parameters.

The atmospheric pressure condition of a laboratory-scale hydrogen production system is 0.1 MPa (= 101.325 kPa), but hydrogen production systems coupled to a VHTR for mass hydrogen production are assumed to be pressurized in the range of about 5–7 MPa. The cell potential decreases with system pressure under the same current density conditions, as shown in **Fig. 9**.

(2) Effect of Molar Flow Rate

Changes to the H_2 (or H_2O) molar fraction at the inlet affect both the molar flow rate for production at the outlet and V_{nernst} potential. Initial conditions for molar flow rate analysis are as follows:

– Inlet flow rate at the cathode: 1.0 gmole/s (mole fractions: H_2O-90%, H_2-10%),
– Inlet flow rate at the anode: 1.0 gmole/s (mole fractions: O_2-21%, N_2-79%),

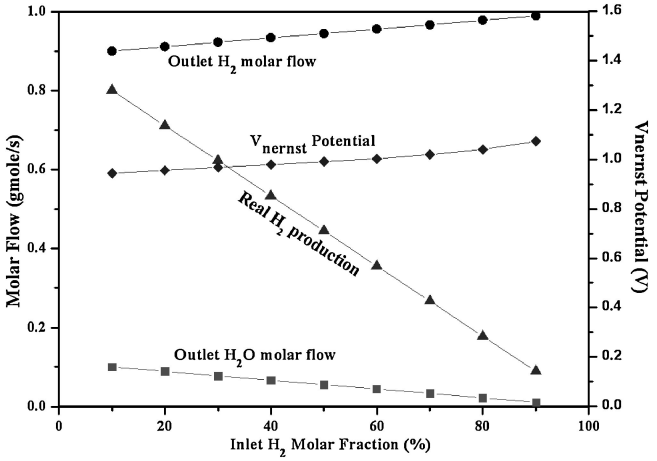

Fig. 10 Outlet molar flow for inlet H_2 molar fraction

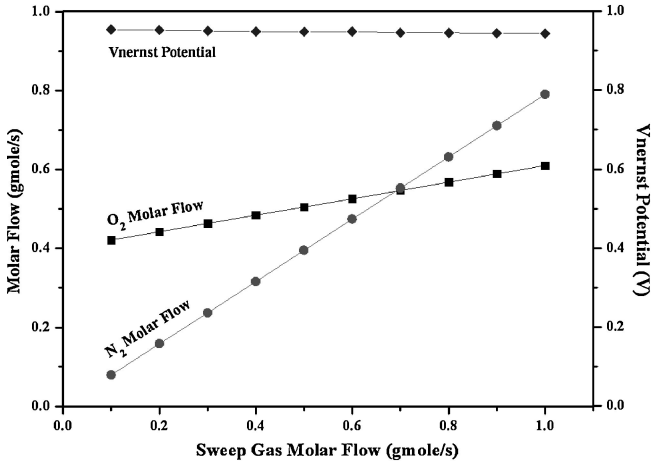

Fig. 11 Outlet molar flow for sweep gas molar flow

– Values for temperature, pressure, current density, and ASR: same as in Table 2.

(a) The H_2 molar fraction for the cathode inlet flow of 1.0 gmole/s is changed from 10 to 90% and the results are shown in **Fig. 10**. Increasing the H_2 molar flow at the inlet causes an increased total H_2 molar flow rate at the outlet, but results in the reduction of real H_2 produced by the electrolysis reaction. The amounts of real H_2 produced can be calculated using Eq. (13). When the inlet H_2 molar fraction increases, V_{nernst} potential increases slightly, and reactions will not happen normally because there exists very little H_2O for electrolysis. When the high-temperature electrolysis experiment occurs, injecting a small fraction of H_2 is helpful in preventing oxidation on the cathode electrode, which is generally a nickel-based material. To prevent oxidation at the cathode electrode and maintain an effective electrolysis reaction, a small fraction (10–20%) of H_2 needs to be blown at the cathode inlet.

$$\text{Real } H_2 \text{ production} = \dot{n}_{o\_H_2} - \dot{n}_{i\_H_2}, \tag{13}$$

where

$\dot{n}_{o\_H_2}$: H_2 molar flow rate at the outlet,

$\dot{n}_{i\_H_2}$: H_2 molar flow rate at the inlet.

Air, which generally consists of 79% nitrogen (N_2) and 21% oxygen (O_2), is used as inlet gas for the anode electrode in the electrolyzer model. Using air as sweep gas at the anode electrode releases oxygen produced by the electrolysis and can be sustainable electrolysis.

(b) The results of changing the anode inlet flow from 0.1 to 1.0 gmole/s are shown in the **Fig. 11**. Increasing the total molar flow rate from 0.1 to 1.0 gmole/s at the anode inlet increased the amount of both O_2 and N_2 molar flows at the anode outlet. When the total molar flow of sweep gas is over 0.7 gmole/s, the molar flow of O_2 is higher than that of N_2. According to the amounts of sweep gas, O_2 and N_2 molar flows at the outlet vary. If molar flow rates of sweep gas are higher than those of H_2 and H_2O in the inlet, the molar flow rate of O_2 in the outlet will increase, as shown in Fig. 11.

(3) Carrier Gas Effect

An inert gas, such as nitrogen or argon, was used as a carrier gas in the HTE experiment. Independent variations in both the partial pressure and flow rates for H_2 and H_2O are permitted because carrier gas is used.[15] The initial conditions for analyzing carrier gas effects are as follows:

– Inlet flow rate at the cathode: 1.0 gmole/s (mole fractions: H_2O-90%, H_2-10%, N_2-0%),
– Inlet flow rate at the anode: 1.0 gmole/s (mole fractions: O_2-21%, N_2-79%),
– Values for temperature, pressure, current density, and ASR: same as in Table 2.

Table 3 Changes in molar fraction at the cathode inlet

Molar fraction			Molar flow rate (total, gmole/s)
H_2O	H_2	N_2	
0.90	0.10	0.00	1.00
0.81	0.09	0.10	1.00
0.72	0.08	0.20	1.00
0.63	0.07	0.30	1.00
0.54	0.06	0.40	1.00
0.45	0.05	0.50	1.00

When the molar fraction of nitrogen at the cathode inlet increases from 0 to 50%, as shown in **Table 3**, the molar flow of hydrogen is reduced and the cell potential decreases from 1.01 to 1.006 V, as shown in **Fig. 12**. Based on experiments, carrier gas is helpful in measuring the hydrogen concentration or calculating produced hydrogen amounts at the cathode outlet. The carrier gas was therefore injected at the cathode inlet and the use of a lower amount of carrier gas is recommended.

(4) Electrolysis Conversion Rate Effect

As indicated above, a simulated chemical reaction is used as the conversion reactor model in the middle of an HYSYS reactor type. To use the conversion reactor model, the stoichiometry information (ex. $H_2O \rightarrow H_2 + 1/2O_2$) for water electrolysis and conversion rate are needed. The conversion rate describes the percentage of water being split in the electrolyzer model.

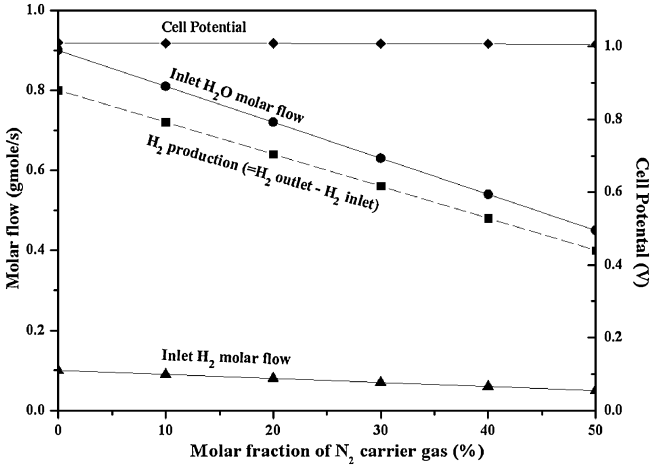

Fig. 12 Molar flow and cell potential for carrier gas

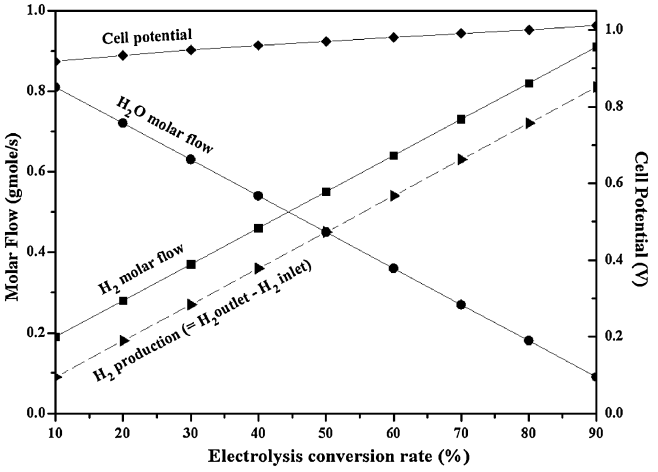

Fig. 13 Molar flow for electrolysis conversion rate

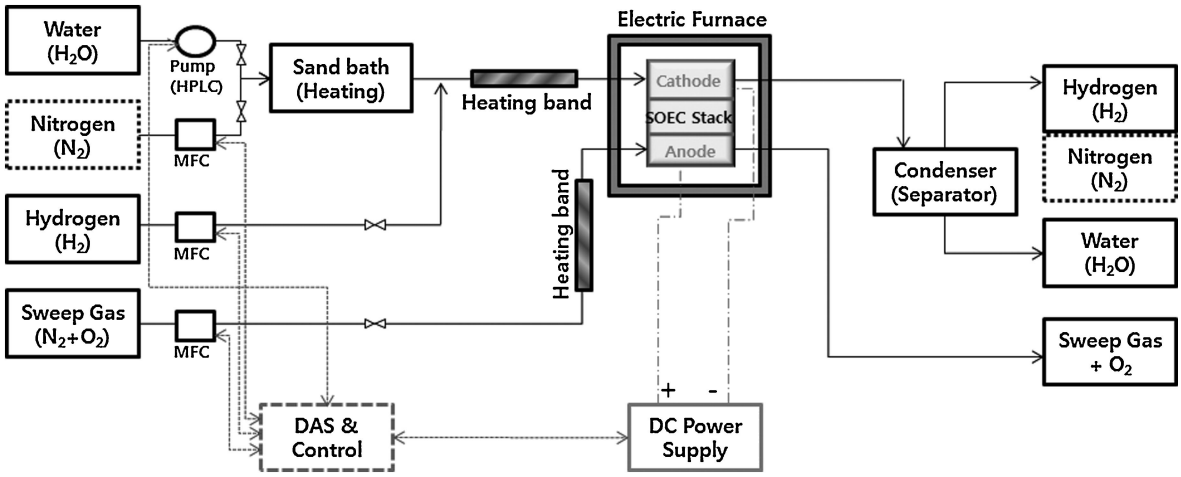

Fig. 14 Concept of HTES using solid oxide electrolysis cell

The assumed calculation is the same as in Table 2, but the electrolysis conversion rate varies from 10 to 90%. The effects of the conversion rate are shown in the **Fig. 13**. When the electrolysis conversion rate is increased, both hydrogen production and cell potential increase, but the H_2O molar flow is less because of the increased conversion rate. The higher conversion rate in the isothermal electrolysis reaction is therefore recommended to maximize hydrogen production.

III. Simulation of an HTES Coupled with a VHTR

The developed electrolyzer model can be used to analyze or design the HTES using the SOEC system. By using the SOEC, the HTES consists of high-temperature electrolysis parts (including an electric furnace and solid oxide electrolysis cell stack, pipe system for gases, and data acquisition system), a control system, a power supply, and a heating and cooling system as shown in **Fig. 14**. The solid oxide electrolysis cell stack is made of a cathode, an anode, an electrolyte, an interconnector, and upper and bottom plates.

The newly developed HYSYS electrolyzer component described in the previous sections was used to analyze the HTES integrated with a VHTR. **Figure 15** shows the simplified hydrogen production system coupled with a very high temperature reactor. Inlet and outlet temperatures were assumed to be 490 and 900°C, respectively, and the hydrogen production rate for the 600 MWth was assumed to be 2.125 kg/s (2.68×10^6 tonne/yr for 4×600 MWth).[16] The required process heat and electrical work were about 32.5 and 200.6 MWth, respectively. The overall efficiency of the system was estimated to be 35.98% from Eq. (14),

$$\eta = \frac{\sum W_T - \sum W_C - \sum W_{CIR} - \sum W_{HTE} + Q_{H_2}}{Q_{th}}, \tag{14}$$

where

η: overall system efficiency,
$\sum W_T$: turbine work,
$\sum W_C$: total compressor work,
$\sum W_{CIR}$: circulator work,
$\sum W_{HTE}$: total work required for high-temperature electrolysis,
$\sum Q_{H_2}$: H_2 production rate × lower heating value (242 kJ/mol),
$\sum Q_{th}$: reactor thermal power.

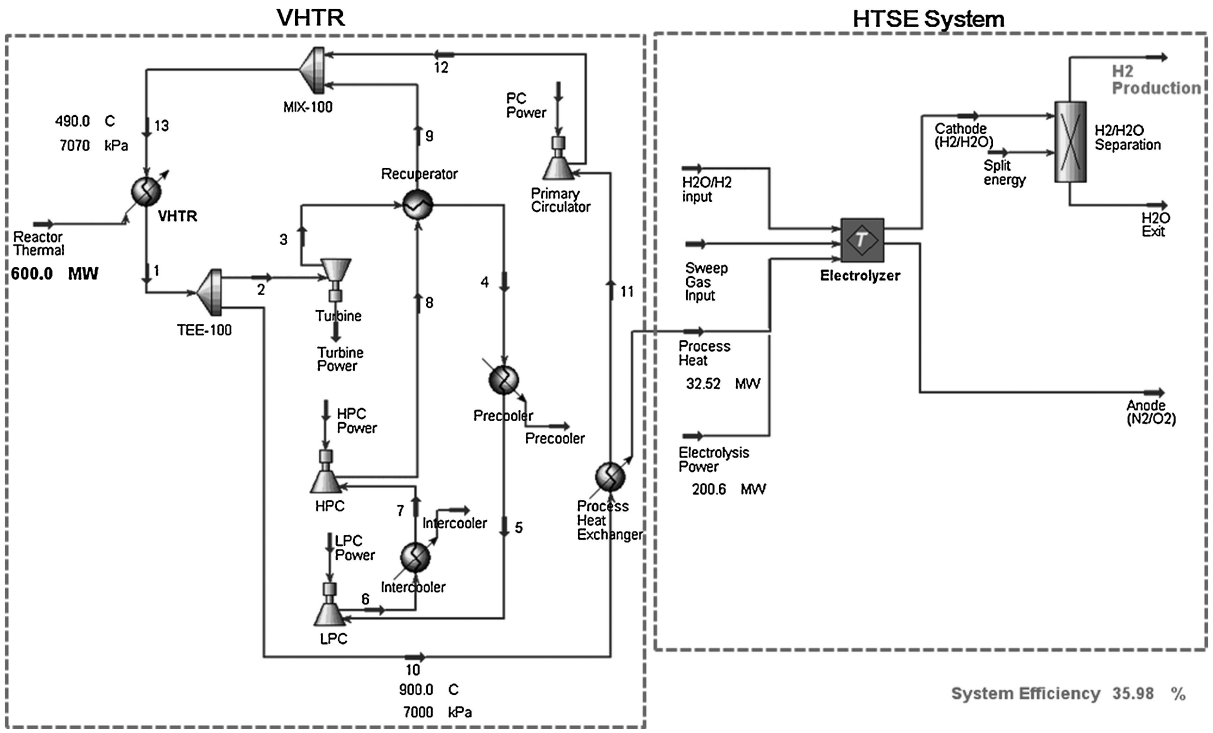

Fig. 15 Process flow diagram of hydrogen production system coupled with VHTR (HYSYS)

IV. Conclusions

Based on the thermodynamics of high-temperature electrolysis, an electrolyzer model was developed for use in analyzing the hydrogen production system. A sensitivity analysis was then carried out for the principal effective parameters: temperature, pressure, current density, area-specific resistance, flow rate in the inlet, and fraction of carrier gas or sweep gas. The analysis results show that cell potential increases with increasing current density or area-specific resistance and decreases with increasing temperature. An increased hydrogen molar flow causes an increased total hydrogen molar flow rate at the outlet, but results in a reduction of real hydrogen production. If the molar flow rate of sweep gas is higher than that of hydrogen and steam at the inlet, the molar flow rate of oxygen is reduced at the outlet. When the molar fraction of nitrogen increases from 0 to 50%, it reduces the molar flow of hydrogen and slightly lessens the cell potential. The HTES system coupled with a VHTR was then modeled and analyzed using the newly developed HYSYS electrolyzer model. The overall efficiency of the system was then estimated to be about 35.98%. However, further studies are required to optimize configurations and efficiency of the hydrogen production system.

Acknowledgements

The work described in this paper was supported by the Korea Hydraulic & Nuclear Power Company, Korea.

References

1) National Research Council and National Academy of Engineering, *The Hydrogen Economy: Opportunities, Costs, Barriers, and R&D Needs*, The National Academies Press, Washington, D.C. (2004).
2) *Nuclear Hydrogen R&D Plan*, Office of Nuclear Energy, Science and Technology, U.S. Department of Energy (2004).
3) S. C. Singhal, K. Kendall, *High Temperature Solid Oxide Fuel Cells: Fundamentals, Design and Applications*, Elsevier Ltd. (2003).
4) *Aspen HYSYS Ver. 7.0: User's Guide*, Aspen Technology, Inc. (2008).
5) C. H. Oh, E. S. Kim, S. R. Sherman, R. Vilim, *HyPEP FY-07 Report: Initial Calculations of Component Sizes, Quasi-static, and Dynamics Analyses*, INL/EXT-07-12937, Idaho National Laboratory (2007).
6) M. G. McKellar, J. E. O'Brien, E. A. Harvego, J. S. Herring, *Optimized Flow Sheet for a Reference Commercial-Scale Nuclear-Driven High-Temperature Electrolysis Hydrogen Production Plant*, INL/EXT-07-13573, Idaho National Laboratory (2007).
7) J. E. O'Brien, "Thermodynamic considerations for thermal water splitting processes and high temperature electrolysis," *Proc. 2008 Int. Mechanical Engineering Congress and Exposition*, Boston, USA, Oct. 31–Nov. 6, 2008, IMECE2008-68880 (2008).
8) B. Yildiz, J. Smith, T. Sofu, *Thermal-Fluid and Electrochemical Modeling and Performance Study of a Planar Solid Oxide Electrolysis Cell: Analysis on SOEC Resistances, Size, and Inlet Flow Conditions*, ANL-06/52, Argonne National Laboratory (2006).
9) D. Grondin, J. Deseure, A. Brisse, M. Zahid, P. Ozil, "Multiphysics and simulation of a solid oxide electrolysis cell," *Proc. COMSOL Conf.*, Hannover, Germany (2008).

10) J. A. Dean, *Lange's Handbook of Chemistry Fifteenth Edition*, McGraw-Hill, Inc. (1999).
11) G. M. Masters, *Renewable and Efficient Electric Power Systems*, Wiley-Interscience, John Wiley & Sons, Inc., New Jersey, 212 (2004).
12) Y. J. Shin, W. Park, J. H. Chang, J. K. Park, "Evaluation of the high temperature electrolysis of steam to produce hydrogen," *Int. J. Hydrogen Energy*, **32**, 1486–1491 (2007).
13) L. Mingyi, Y. Bo, X. Jingming, C. Jing, "Thermodynamic analysis of the efficiency of high-temperature steam electrolysis system for hydrogen production," *J. Power Sources*, **177**, 493–499 (2008).
14) L. Sandell, *High Temperature Gas-Cooled Reactors for the Production of Hydrogen: Establishment of the Quantified Technical Requirements for Hydrogen Production That Will Support the Water-Splitting Processes at Very High Temperatures*, EPRI Technical Report 10096874, Electric Power Research Institute (EPRI), 3–43 (2004).
15) J. S. Herring, *High-Temperature Electrolysis*, DOE Hydrogen Program, FY 2005 Progress Report (2005).
16) D. S. Vandel, S. Bader, *NGNP Engineering White Paper: By-Products Trade Study*, INL/EXT-07-12728, Idaho National Laboratory, Next Generation Nuclear Plant Project, 4 (2007).